



Impact of Dufour and Thermal Radiation on Unsteady MHD Blood Flow through Bifurcated Arteries with Heat Source and Chemical Reaction

Yusuf Ya'u Gambo¹, Bashir Ya'u Haruna^{2*}, Auwalu Alhassan Girema³ and Mustapha Balogun⁴

^{1, 2, 3 & 4}Department of Mathematics, Northwest University, Kano, Kano State, Nigeria.

*Corresponding Author Email: by.7haruna@gmail.com



ABSTRACT

The analytical study of heat and mass transfer on magnetohydrodynamic (MHD) blood flow through bifurcated arteries under influence of an inclined magnetic field with thermal radiation and chemical reaction in the presence of Dufour effect has been investigated. The induced magnetic and electric fields generated by the blood are assumed to be negligible due to the low magnetic Reynolds number. The dimensionless system of governing equations was solved analytically with appropriate boundary conditions. The regular perturbation theory has been utilized to obtain the analytical solution for velocity, temperature and molar species of biofluid (blood). The validation of the analytical method was found suitable by obtaining numerical solutions with MATLAB and compared with the analytical results. The influence of Dufour number, magnetic field parameter, heat source parameter, Prandtl number, thermal radiation, Schmidt number and chemical reaction are discussed in details. Dual solutions for the axial velocity, temperature distribution, concentration profile, local skin coefficient, Nusselt number and Sherwood number were presented graphically for realistic values of Pr and Sc as well as for arbitrary values of other parameters. The behaviour of primary parameter has been notably observed that the temperature variation was strongly dependent on concentration gradient due to the presence of Dufour effect. An increase in magnetic field and thermal radiation reduces the blood velocity within the arterial layers by generating a Lorentz force. An increase in Dufour number corresponds to lower molecular diffusivity due to the dispersal momentum diffusivity that leads to rise temperature gradient.

Keywords:

MHD flow,
Dufour effect,
Chemical reaction,
Thermal radiation,
Heat source.

INTRODUCTION

Many authors have conducted extensive research studies in biofluids in the past few decades, with a particular focus on the theoretical impact of magnetohydrodynamics (MHD). MHD involves the investigation of the flow of electrically conducting fluids under the influence of a magnetic field. In the situation of human physiology, MHD can be employed to modulate blood flow rates in the arterial system. This approach holds promise in the treatment of cardiovascular conditions where accelerated blood flow, such as in hypertension and hemorrhages, exacerbates the disease. Mathematical analysis for a viscous, Newtonian blood flow through a bifurcated artery with the influence of magnetic field is carried out by (Sharma *et al.*, 2004; Singh and Rathee, 2010; Eldesoky *et al.*, 2019; Srinivasacharya and Rao, 2016; Shit and Roy, 2016; Hamza *et al.*, 2024). The studies specifically investigated the impact of MHD flow in bifurcated arteries under the influence of a magnetic field with heat source. Authors in (Verma and Parihar, 2009;

Sanyal and Biswas, 2010) described that the electromagnetic force (Lorentz force) acted upon an artery which resisted its motion and impeded blood.

This resistance could be harnessed for treating conditions such as cardiovascular diseases where accelerated blood circulation is a concern. Authors like Tzirtzilakis (2005); Korchevskii and Marochnik (1965) developed mathematical model of bio-magnetic fluid dynamics (BFD) which made a description of the Newtonian blood flow under the action of magnetic field. This model was consistent with the principles of magnetohydrodynamic effect on blood flow which was integrating magnetization and electrical conductivity of blood. They considered blood as Newton fluid in their exploration of blood flow. The studies on the effect of MHD blood flow in the presence of heat source were described by (Sanyal *et al.*, 2007; Ramamurthy *et al.*, 1994; Das *et al.*, 2009) that the alteration in heat source was accelerated the temperature of the fluid flow.

Combined heat and mass transport phenomena in the

human body have been paid attention for the examination of their effects by many authors. One of the three thermal mechanisms through which heat transfer can occur is convection, conduction or radiation while mass transfer is the net movement of mass from one position to another. Mass transfer can be found in many processes, such as evaporation, drying etc. Chakravarty and Santabrata (2005) investigated the influence of transport phenomena on blood flow through a bifurcated artery. Jamali *et al.* (2019) studied heat transfer simulation on blood flow through a stenosed bifurcated artery by considering blood as Newtonian fluid and revealed that the presence of stenosis with slightly change of the stenosis shape and value of Reynold number influenced to the velocity, temperature distribution and reverse flow re-circulation as indicated by negative flow near the arterial wall. Latha and Kumar (2016) focused on to discussing the effect of mass transfer on the flow of blood through parallel plate channel with radiation and heat source. Adhikary and Misra (2011) addressed the oscillatory flow of fluid and heat transfer in a porous oscillating channel with an external magnetic field while Lagendijk (1982) explored the influence of blood flow in large vessels on temperature distribution in hyperthermia. Suri and Suri (1981) proposed study of static magnetic field effect on blood flow through a bifurcated artery. Authors examined how a high magnetic field on blood flow rate, discovering that it induces a minor blockage. Eldesoky (2012) extended a model by Jain *et al.* (2009) with heat source. He mentioned heat source is capable to accelerate the blood flow and temperature distribution of the flowing region. Wang (2008) modelled blood flow in small tubes using a two-fluid model with fully developed constant heat flux and convective heat transfer.

The analysis of thermal radiation and chemical reactions is closely associated with a variety of exothermic and endothermic processes. This interaction is particularly important in arterial blood flow, where the combined effects of thermal radiation and chemical reactions facilitate in describing internal flow within arteries. Such phenomena are especially relevant in medical applications. Furthermore, chemical reaction effects significantly influence transport processes, which are influenced by the combined action of buoyancy forces arising from thermal and mass diffusion. The effects of heat source and thermal radiation on MHD blood flow in a stenosed tapered artery has been investigated by (Omamoke *et al.*, 2020; Kumar *et al.*, 2021; Ahmed *et al.*, 2023) conducted a corresponding analysis of a bio-magnetic fluid flow by the application of inclined magnetic force for the treatment of tumours.

Several studies reveal that heat and mass transfer flow can be affected by diffusion-thermo. Convection becomes complicated when concentration and temperature occur simultaneously resulting to the effects of diffusion-thermo and thermal-diffusion. Diffusion thermo refers to the

phenomenon when heat transfer is generated by concentration gradients in a fluid is termed as Dufour effect. This effect arises when heat and mass transfer interact simultaneously having an effect on different physical properties within a moving dynamical fluid. In Platten (2006); Reddy (2016); Hayat *et al.* (2012); Shukla *et al.* (2022) described the thermal diffusion caused by variations in the concentration of components within the fluid. A Mathematical Analysis made by Eckert and Drake Jr (1987) on heat and mass transfer. Authors particularly reported the considerable impact of the Dufour effect which cannot be neglected in analyses pertaining heat transfer. Jha and Gambo (2019) discussed an analytical approach on unsteady free convection and mass transfer flow past an impulsively started vertical plate with Soret and Dufour effects. Mishra and Nidhish (2023) investigated the effects of Soret and Dufour on MHD nanofluid flow of blood through a stenosed artery with variable viscosity. An investigation made by. Sharma *et al.*, (2019) studied Soret and Dufour effects on bio-magnetic fluid of blood flow through a tapered porous stenosed artery.

A survey of literature revealed a numerous of authors have paid attention to the effect of diffusion-thermo phenomenon. However, there seems to be no literature with Dufour effect on MHD blood flow through bifurcated arteries. Therefore, the current investigation is concerned with the influence of Dufour effect, thermal radiation, chemical reaction and heat source on unsteady MHD blood flow passing through bifurcated arteries along with impact of an inclined magnetic field to the artery. It will help in the treatments of carotid body tumour, strokes and pain resulting from sickle cell anaemia and the treatment of low blood pressure, using magnetic field normal and also treatment of tumours with thermal radiation.

The non-dimensionalisation of parameters in the system of equations is presented in the Material and Methods section. In the Method of Solution, the model equations are solved analytically using a regular perturbation theory. In the Results and Discussions section, computations are presented graphically to analyse the behaviour of fluid (blood) velocity, temperature, concentration as well as local skin friction, Nusselt number and Sherwood number. The Results and Discussions section outlines the key conclusions drawn from the present study. Some parameterized constants are provided in the Appendix.

MATERIALS AND METHODS

Consider the artery configuration through an asymmetrical bifurcation about x -axis as shown in Figure (1), which illustrates the blood flow between two electrically nonconducting infinite horizontal plates ideally located at $y = \pm 1$. The mass flow rate at

any cross-section normal to the flow direction is expressed as $m = 2d\rho\bar{v}$, where $2d$ is the channel width, ρ is the blood density and \bar{v} represents the mean velocity of a fluid. The angle of bifurcation is about zero due to the division of a parallel plate channel into two separate streams. The wall thickness at the bifurcated region is assumed to be negligibly small that the rate of mass flow in any cross-section of bifurcated regions to be represented by $m/2$.

This exploration contemplates a time-dependent MHD blood flow within a parallel channel wall embedded in a porous medium. The flow is subjected to a uniform

magnetic field applied transversely to the flow direction. Thus, porous medium is homogeneous and isotropic and the induced magnetic and electric fields generated by the blood are deemed negligible due to the low magnetic Reynolds number $Re = \rho\bar{v}/\mu$, which implies that their influence on the flow is minimal (Necatti, 1986). Blood is treated as a Newtonian, incompressible, homogeneous and viscous fluid with the constant viscosity throughout the analysis. The Fåhræus–Lindqvist effect is neglected. See Refs. Zamir and Roach (1973), Kumar *et al.*, (2021).

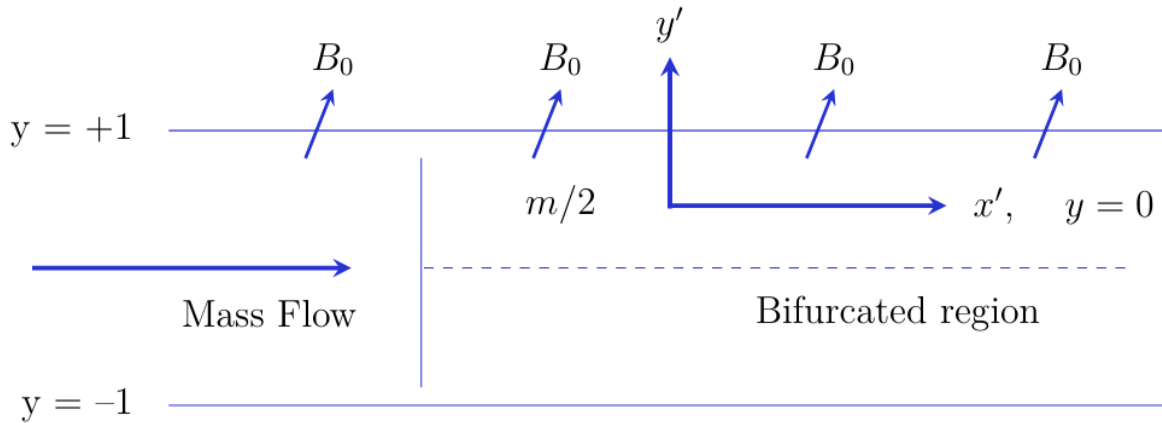


Figure 1: Flow geometry of a bifurcated channel with inclined magnetic fields

Let u' and v' be components of velocity along the Cartesian directions x' and y' respectively at time t' in a flow field. The unsteady-state conservation of momentum, mass, energy and concentration can be described by the following equations (White, 2006)

$$\frac{\partial u'}{\partial t'} + \frac{1}{\rho} \frac{\partial p'}{\partial x'} = \frac{\mu}{\rho} \frac{\partial^2 u'}{\partial y'^2} - \frac{u'}{K} - \frac{\sigma B_0^2 \sin^2 \varphi}{\rho} u' + g\beta(T' - T'_0) + g\beta^*(C' - C_0) \tag{1}$$

$$\frac{\partial u'}{\partial x'} + \frac{\partial v'}{\partial y'} = 0, \tag{2}$$

$$\frac{\partial T'}{\partial t'} = \frac{k}{\rho c_p} \frac{\partial^2 T'}{\partial y'^2} + \frac{Q}{\rho c_p} (T' - T'_0) + D^* \frac{\partial^2 C'}{\partial y'^2} - \frac{\partial q_r}{\partial y'}, \tag{3}$$

$$\frac{\partial C'}{\partial t'} = D_m \frac{\partial^2 C'}{\partial y'^2} - k_1(C - C_0), \tag{4}$$

The third and last terms in equation (3) corresponds to the Dufour parameter and the radiative heat flux respectively. The induced radiative heat transfer is given by $q_r = (4\delta/3k')(dT'^4/dy')$. In the blood vessel, both T and T_0 are sufficiently high and their difference is large enough to induce radiative heat transfer. This is based on the fact that at elevated temperatures, radiation becomes a significant mode of heat transfer. The temperature

difference is expressed as $T' = 4T_0^3 T - 3T'$ where T'_0 represents the ambient temperature. This is derived from the Roseland approximation for radiative heat transfer which simplifies the Stefan-Boltzmann equation under conditions of high temperature gradients. Thus, the radiative heat transfer is given by $q_r = (16\delta T_0^3/3k')(dT'/dy')$, where k' indicates the Roseland mean absorption coefficient and δ is the Stefan-Boltzmann constant.

In equation (4), D_m is the diffusion coefficient and the last term represents the reaction rate, where k_1 denotes the rate of drug diffusion across the affected region. This equation is used to determine the level of drug concentration in the affected region. Ref. Granot and Rubinsky (2008).

The appropriate boundary conditions are Latha and Kumar (2016); Prakash *et al.*, (2011):

$$\begin{aligned} \phi' = e^{-\gamma^2 t}, \quad \theta' = e^{-\gamma^2 t}, \quad u' = e^{-\gamma^2 t}, \quad v' = e^{-\gamma^2 t} \quad \text{at } y' = -1 \\ \phi' \rightarrow 0, \quad \theta' \rightarrow 0, \quad u' \rightarrow 0, \quad v' \rightarrow 0, \quad \text{at } y' = +1 \end{aligned} \tag{5}$$

Introducing the following dimensionless variables

$$\left\{ \begin{aligned} x' = \frac{x}{a}, \quad u' = \frac{u}{\left(\frac{m}{2d\rho}\right)}, \quad \phi' = \frac{\phi(2d^3\rho^2)}{m\mu}, \quad f(x, t) = \frac{(\partial p/\partial x)}{(m\mu/2d^3\rho)}, \\ y' = \frac{y}{a}, \quad v' = \frac{v}{\left(\frac{m}{2d\rho}\right)}, \quad \theta' = \frac{\theta(2d^3\rho^2)}{m\mu}, \quad t' = \frac{t}{(d^2\rho/\mu)}, \quad \eta = \frac{\mu}{\rho} \end{aligned} \right. \tag{6}$$

Equations (1)-(4) are transformed into dimensionless forms by equation (6), then the model equations of motion are given by:

$$\frac{\partial u}{\partial t} + f = \frac{\partial^2 u}{\partial y^2} - \left(M^2 \sin^2 \varphi + \frac{1}{n_p} \right) u + g\beta\theta + g\beta\phi, \quad (7)$$

$$\frac{\partial u}{\partial x} + \frac{\partial v}{\partial y} = 0, \quad (8)$$

$$\frac{\partial \theta}{\partial t} = \left(\frac{1}{\eta Pr} + R \right) \frac{\partial^2 \theta}{\partial y^2} + \frac{H}{\eta Pr} \theta + \frac{D_f}{\eta Pr} \frac{\partial^2 \phi}{\partial y^2}, \quad (9)$$

$$\frac{\partial \phi}{\partial t} = \frac{1}{Sc} \frac{\partial^2 \phi}{\partial y^2} - C_l \phi, \quad (10)$$

where,

$$\left\{ \begin{array}{l} Pr = \frac{\mu c_p}{k}, \quad Sc = \frac{\mu}{\rho D_m}, \quad D_f = \frac{D^* k}{\mu c_p}, \quad H = \frac{Q d^2}{k} \\ M^2 = \frac{\sigma B_0^2 d^2}{\rho}, \quad R = \frac{16 \delta^* T_0^3}{3 \eta k}, \quad C_l = \frac{\rho d^2 k_1}{\mu}, \quad n_p = \frac{\kappa \rho d^2}{\mu} \end{array} \right\}.$$

Method of Solution

In order to derive analytical solutions to equations (7)-(10) subject to the boundary condition, the regular perturbation method is applied to take the forms as

$$u(y, t) = u_0(y) e^{-\gamma^2 t}, \quad (11)$$

$$v(y, t) = v_0(y) e^{-\gamma^2 t}, \quad (12)$$

$$\theta(y, t) = \theta_0(y) e^{-\gamma^2 t}, \quad (13)$$

$$\phi(y, t) = \phi_0(y) e^{-\gamma^2 t}, \quad (14)$$

Equation (5) is reduced to

$$\left. \begin{array}{l} \phi_0 = 1, \quad \theta_0 = 1, \quad u_0 = 1, \quad v_0 = 1 \quad \text{at } y = -1 \\ \phi_0 = 0, \quad \theta_0 = 0, \quad u_0 = 0, \quad v_0 = 0 \quad \text{at } y = +1 \end{array} \right\} \quad (15)$$

In view of equations (11)-(14), equations (7)-(10) reduce to

$$\frac{\partial^2 u_0}{\partial y^2} + a_3^2 u_0 = \hbar - g\beta\theta_0 - g\beta'\phi_0, \quad (16)$$

$$v_0 = a_2, \quad (17)$$

$$\frac{\partial^2 \theta_0}{\partial y^2} + a_8^2 \theta_0 = -a_5 \frac{\partial^2 \phi_0}{\partial y^2}, \quad (18)$$

$$\frac{\partial^2 \phi_0}{\partial y^2} + a_7^2 \phi_0 = 0. \quad (19)$$

Equation (11) yields the blood velocity in the direction of axial flow

$$u(y, t) = \left[\begin{array}{l} a_{15} - a_{16} \cos a_7 y + a_{17} \sin a_7 y - a_{18} \cos a_8 y \\ \quad + a_{19} \sin a_8 y \\ - a_{20} \cos a_7 y + a_{21} \sin a_7 y + a_{22} \cos a_9 y \\ \quad - a_{23} \sin a_9 y \end{array} \right] e^{-\gamma^2 t} \quad (20)$$

As given by equation (12), the blood velocity through the artery normal to the flow is described as

$$v(y, t) = a_2 e^{-\gamma^2 t} \quad (21)$$

From equation (13), the temperature field in the arterial blood yields

$$\theta(y, t) = [a_{11} \cos a_7 y - a_{12} \sin a_7 y + a_{13} \cos a_8 y - a_{14} \sin a_8 y] e^{-\gamma^2 t} \quad (22)$$

The concentration profile is given by equation (14), we obtain

$$\phi_0(y) = \left[\frac{\cos a_7 y}{2 \cos a_7} - \frac{\sin a_7 y}{2 \sin a_7} \right] e^{-\gamma^2 t} \quad (23)$$

The local skin friction coefficient (C_f), Nusselt number (Nu) and Sherwood number (Sh) are dimensionless quantities that indicate the rates of momentum, heat and mass transfers process respectively. These quantities are utilized to investigate the boundary layer behaviour in blood flow and convective transport phenomena. The local skin friction, along with the Nusselt number and Sherwood number will be computed at the upper wall of the bifurcated region where $y = -1$.

$$C_f = -\mu \left(\frac{\partial u}{\partial y} \right)_{y=-1}, \quad (24)$$

$$Nu = \left(\frac{\partial \theta}{\partial y} \right)_{y=-1}, \quad (25)$$

$$Sh = \left(\frac{\partial \phi}{\partial y} \right)_{y=-1}, \quad (26)$$

Local Skin Friction Coefficient:

Thus, the local skin friction is obtained by (24) as follows

$$C_f = \mu \left[\begin{array}{l} a_{16} a_7 \sin a_7 y - a_{17} a_7 \cos a_7 y + a_{18} a_8 \sin a_8 y \\ \quad - a_{19} a_8 \cos a_8 y \\ + a_{20} a_7 \sin a_7 y - a_{21} a_7 \cos a_7 y + a_{22} a_9 \sin a_9 y \\ \quad - a_{23} a_9 \cos a_9 y \end{array} \right] e^{-\gamma^2 t} \quad (27)$$

Heat Transfer Coefficient:

The dimensionless form for the rate of heat transfer coefficient at the lower wall of the bifurcation in terms of the Nusselt number is defined by (25) as

$$Nu = [a_{11}a_7\sin a_7 - a_{12}a_7\cos a_7 + a_{13}a_8\sin a_8 - a_{14}a_8\cos a_8]e^{-\gamma^2 t} \quad (28)$$

Mass Transfer Coefficient:

The rate of mass transfer coefficient at the lower wall of the bifurcation in terms of the Sherwood number is given by equation (26) as

$$Sh = -a_7 \left[\frac{\cos 2a_7}{\sin 2a_7} \right] e^{-\gamma^2 t} \quad (29)$$

In order to benchmark the integrity of the current analytical approach, a methodical comparative study has been instigated in conjunction with the prior investigations carried out by Ahmed *et al.*, (2023) and Eldesoky (2012) and found them in excellent agreement as demonstrated in Table 1 and Table 2, respectively. These tables corroborate that the adopted flow model is robustly validated and lends itself to further exploration through a variety of distinct physical parameters.

Validation and Accuracy

Table 1: Distribution of axial velocity for R , M , C_l , Sc and t with mass flux at $\gamma = 1$, $f = 0.5$, $\eta = 0.1$, $t = 1$, $Sc = 0.5$, $Pr = 0.7$, $H = 0.1$, $D_f = 0$, $g = 1.5$, $\beta = 0.5$ and $\beta_0 = 0.5$.

y	R	M	C_l	Sc	t	Ahmed et al. (2023)	Present work
-1.00	0.00	0.10	0.10	0.25	0.00	1.00000	1.00000
-0.50	0.20	0.10	0.10	0.25	0.20	1.04580	1.04050
-0.25	0.20	0.10	0.10	0.50	0.20	1.04570	1.04570
0.00	0.20	0.00	0.00	0.50	0.20	0.94164	0.94164
0.25	0.50	0.50	0.20	0.78	0.40	0.56401	0.56401
0.50	0.50	0.50	0.20	0.78	0.40	0.38188	0.38188
1.00	0.50	0.50	0.20	0.78	0.40	0.00000	0.00000

Table 2: Distribution of temperature field for H , Pr and R without mass flux at R , H , and Pr with mass flux at $\gamma = 0.3$, $\eta = 0.1$, $t = 2$, $D_f = R = 0$

H	Pr	Eldesoky (2012)	Present work
0.2	0.7	0.33654	0.33654
0.2	0.7	0.33654	0.33654
0.2	0.7	0.33654	0.33654
0.5	7.0	0.34669	0.34669
0.5	7.0	0.34669	0.34669
0.5	7.0	0.34669	0.34669

In Table 1, the velocity of the bio-fluid is attenuated by the opposing influence of the magnetic drag force, whereas the Prandtl number serves to shrink the velocity, whereas the reduction in axial velocity is slightly due to a time elapse.

In Table 2, an increase in heat source induces an overshoot in temperature, while a rise in the Prandtl number leads to a corresponding elevation in temperature. In the other hand, it is observed that an elevation in the radiation results in a diminution of temperature. In the absence of Dufour number, the present work has a good agreement with Eldesoky (2012).

RESULTS AND DISCUSSION

The authors systematically scrutinized the effects of the Dufour phenomenon and thermal radiation along with the influences of heat source, chemical reactions in the presence of inclined magnetic fields. Dual results have been computed for axial velocity, temperature distribution, concentration profile, skin friction, Nusselt number and Sherwood number as a function of various governing parameters. The Dufour number (D_f), chemical reaction parameter (C_l), Prandtl number (Pr), Schmidt number (Sc), heat source parameter (H), magnetic parameter (M), decay parameter (γ), radiation parameter (R) and time (t). The magnitudes of Prandtl number (Pr) are nominated for air ($Pr = 0.7$) at 20°C, pure water ($Pr = 7.0$). Similarly, the values of the Schmidt number (Sc) are chosen for water-vapour ($Sc = 0.60$). The identified parameters are set default at $\psi = 0.75, \gamma = 0.1, f = 0.5, \eta = 0.25, t = 1, Sc = 0.5, Pr = 0.7, R = 0.5, M = 0.5, D_f = 0.1, \mu = 0.5, C_l = 0.5, g = 1.5, \beta = 0.5$ and $\beta_0 = 0.5$.

The solutions for the governing equations are graphically reported in Figures (2)-(16).

In Figure (2), the influence of magnetic field parameter (M) and Dufour number (D_f) on the axial velocity. As M increases from $M = 0.25$ to $M = 0.45$, the axial velocity profile decreases for $D_f = 0.10, 0.30, 0.50, 1.00$. Dufour effect is also known as diffusion-thermo effect. By definition, D_f heat generation due to solute concentration gradient.

$D_f = \text{Energy flux due to mass diffusion} / \text{Energy flux due to thermal conduction}$

High values of D_f imply that the solute diffusion contributes significantly to heat transport. While, low values of D_f illustrate that thermal conduction dominates heat transfer. It is indicated that the magnetic field creates a retarding force (Lorentz force), which slows down the motion of the molecules of the blood fluid due to increased resistance. It can also stabilize irregular blood flow caused by arterial branching or irregular geometries. An increasing D_f enhances energy transport in blood which could enhance the delivery of heat-sensitive drugs or reduce thermal gradient.

Figure (3), shows the influence of chemical reaction parameter (C_l) and the Dufour number (D_f) on the axial velocity. Chemical reaction parameter (C_l) quantifies the impact of chemical reactions within the flow. Higher values of C_l correspond to stronger chemical reactions,

which can influence the concentration and velocity profile of the fluid. As C_l increases from $C_l = 0.51$ to $C_l = 0.81$, the axial velocity decreases across the entire transverse range. Strong chemical reaction absorbs energy from the flow, which lead to reduce axial velocity. An increasing D_f raises the axial velocity, especially near the channel centreline ($y = 0$). The enhanced thermo-diffusion D_f supplies additional energy to the flow that counteract viscous force and improve velocity.

Figure (4) displays the impact of the heat source parameter (H) and the Dufour number D_f on the axial velocity $u(y, t)$ across the channel width (y). The increase in H from $H = 0.5$ to $H = 1.5$ enhances the axial velocity. This is because a higher heat source introduces more energy into the biofluid that reduces the viscosity effect and promotes flow acceleration. Heat source (H) could simulate local heat effect such as inflammation. Similarly, increasing the Dufour number D_f enhances axial velocity. A larger D_f signifies more heat being transferred to molecular motion aiding flow of the biofluid.

Figure (5) illustrates the impact of the Dufour number (D_f) and the thermal radiation R on the axial velocity $u(y, t)$. The growing in $D_f = 0.2$ and $D_f = 1.0$ with different values of (R) represented as $R = 0.50, 1.00, 1.50, 2.00$. As D_f increases the axial velocity rises initially (closer to $y = 0$) but decreases more rapidly away from the centreline ($y = \pm 1$). It can be seen that low D_f , radiation has a lesser impact and the flow remains smoother across y while high D_f , the influence of R becomes pronounced with an exaggeration in velocity peak and with steepness in the gradient along y . Since thermal radiation (R) represents the intensity of thermal radiation. Thus, an increasing R consistently raises the peak axial velocity near the centreline ($y = 0$) implying that thermal radiation amplifies the flow speed in the core region. However, the velocity diminishes more steeply as y approaches ± 1 .

In Figure (6), depicts the effects of heat source (H) and Schmidt number (Sc) on axial velocity $u(y, t)$ for $H = 0.5$ to $H = 1.5$ with the variation in Schmidt number $Sc = 1.00, 1.10, 1.20, 1.30$. By definition, heat source (H) represents internal heat generation or absorption in the biofluid when,
 $H > 0$: Heat is being generated (source)
 $H < 0$: Heat is being absorbed (sink)

The Schmidt number (Sc) is defined as the ratio of momentum diffusivity (viscosity) to mass diffusivity and it is particularly useful for characterizing fluid flows where momentum diffusion and mass diffusion occur simultaneously during convection processes. In this study, we consider $H > 0$ so that at $H = 0.5$, the impact of Sc on axial velocity is more moderate, as the biofluid (blood) generates less heat. At $H = 1.5$, the

velocity differences between different Sc values become more pronounced with a reflection of the amplified interaction between heat generation and reduced solute diffusivity.

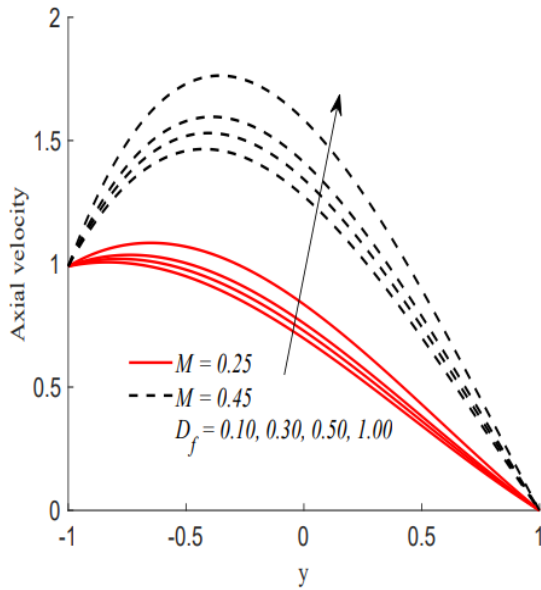


Figure 2: Influence of M, D_f on $u(y, t)$

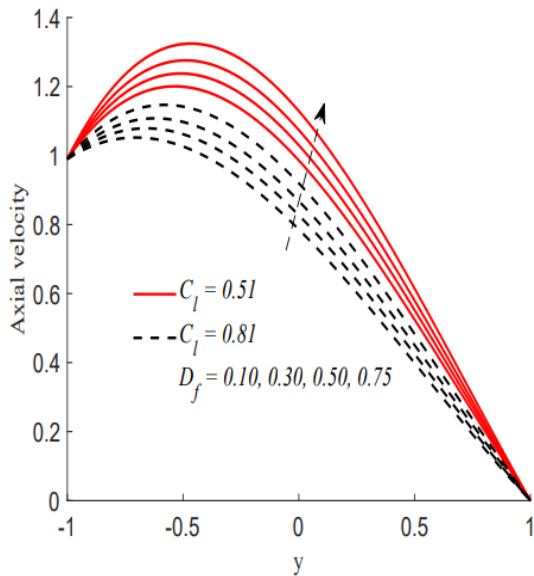


Figure 3: Influence of C_l, D_f on $u(y, t)$

Figure (7) presents the impact of Prandtl number (Pr) and Dufour number (D_f) on temperature distribution $\theta(y, t)$. At higher D_f , the temperature profile rises significantly, but the influence of increasing Pr becomes more noticeable in suppressing the temperature. For lower D_f , the impact of Pr changes is less pronounced due to reduced coupling between diffusion mechanisms. The molecules have freedom to move freely.

In Figure (8), the temperature distribution (θ) for $H = 0.5$ and $H = 1.0$ is plotted with different values of Pr when the parameter $R = 0.2$. It is observed that the influence of

H at higher values lead to an enhancement in the blood flow temperature within the arterial region. Moreover, a similar effect is noticed that when the momentum diffusivity thermal dominates over diffusivity so that the elevation in the biofluid temperature occurs due to higher values of Pr .

In Figure (9), the influence of the Dufour number (D_f) and the Schmidt number (Sc) on the temperature field (θ) is examined for $D_f = 1$ and $D_f = 3.0$ at different values of Sc . It is observed that the level of D_f uplifts, the temperature field increases. As expected, the θ is demonstrated much sufficiency with increasing Sc across region.

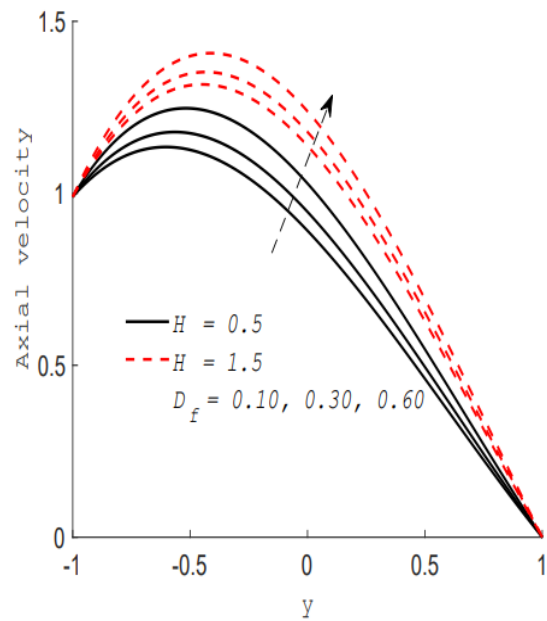


Figure 4: Influence of H, D_f on $u(y, t)$

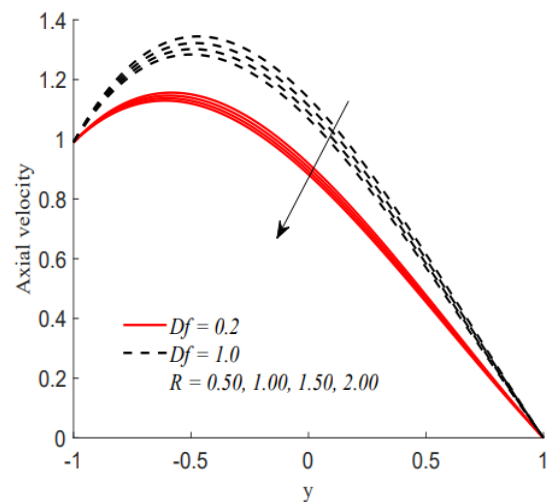


Figure 5: Influence of D_f, R on $u(y, t)$

Figure (10) shows the impact of the chemical reaction parameter (C_l) and the Schmidt number (Sc) on the concentration profile. It can be observed that as C_l increases from $C_l = 0.50$ to $C_l = 1.85$ with the varied Schmidt number ($Sc = 0.00$,

0.50, 0.70, 1.00), the concentration profile decreases more rapidly. As Sc increases, the concentration profile becomes steeper. It illustrates the behaviour that the higher values of Schmidt number which correspond to lower molecular diffusivity lead in greater concentration gradients. Generally, both parameters (C_l and Sc) significantly affect the concentration profile. Higher values of C_l and Sc correspond to faster decay and steeper profiles, respectively.

In Figure 11, It is illustrated that the increase in normal velocity with a higher decay parameter, this shows a more rapid response of the system to transient changes. In physiological terms, a more compliant arterial system or reduced peripheral resistance may lead to faster changes in blood flow velocity after systole. Similar to the system described reaching a saturation point, the cardiovascular system also has limitations. Once arteries are maximally dilated or contractile responses are exhausted, further increases in the decay parameter or other regulatory factors have diminishing effects on blood flow velocity.

Figure (10) shows the impact of the chemical reaction parameter (C_l) and the Schmidt number (Sc) on the concentration profile. It can be observed that as C_l increases from $C_l = 0.50$ to $C_l = 1.85$ with the varied Schmidt number ($Sc = 0.00, 0.50, 0.70, 1.00$), the concentration profile decreases more rapidly. As Sc increases, the concentration profile becomes steeper. It illustrates the behaviour that the higher values of Schmidt number which correspond to lower molecular diffusivity lead in greater concentration gradients. Generally, both parameters (C_l and Sc) significantly affect the concentration profile. Higher values of C_l and Sc correspond to faster decay and steeper profiles, respectively.

In Figure 11, It is illustrated that the increase in normal velocity with a higher decay parameter, this shows a more rapid response of the system to transient changes. In physiological terms, a more compliant arterial system or reduced peripheral resistance may lead to faster changes in blood flow velocity after systole. Similar to the system described reaching a saturation point, the cardiovascular system also has limitations. Once arteries are maximally dilated or contractile responses are exhausted, further increases in the decay parameter or other regulatory factors have diminishing effects on blood flow velocity.

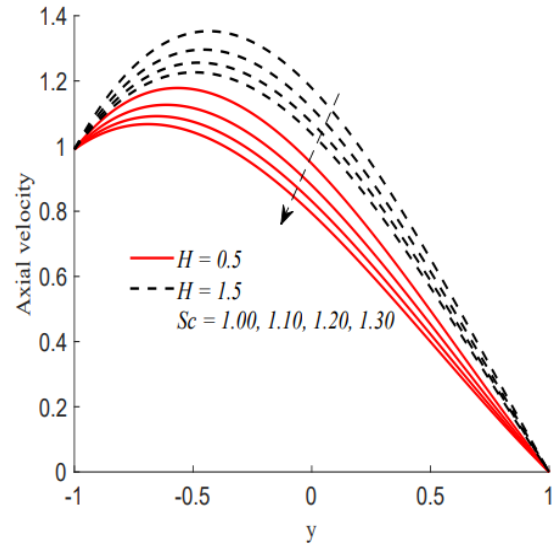


Figure 6: Influence of H, Sc on $u(y, t)$

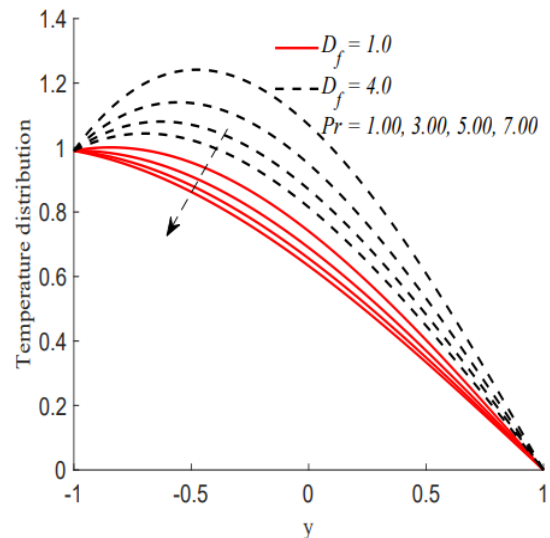


Figure 7: Influence of D_f, Pr on $\theta(y, t)$

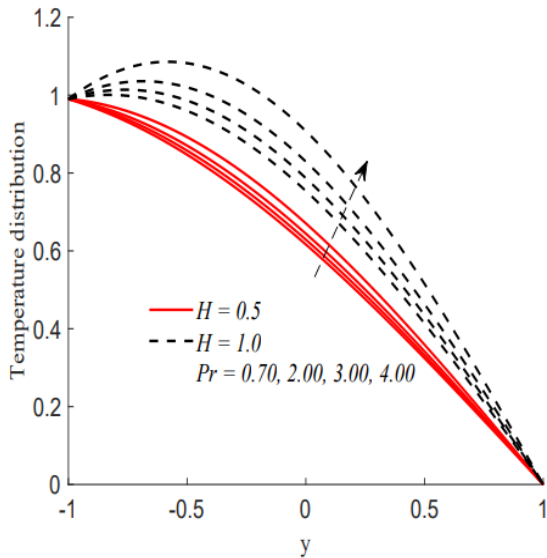


Figure 8: Influence of H, Pr on $\theta(y, t)$

In Figure (12), the behaviour of the Dufour number (D_f), Schmidt number (Sc) and time (t) on the coefficient of skin friction (C_f) for $D_f = 0.2$ and $D_f = 0.6$ with varying values of Sc is plotted having the parameters, $H = 0.5, R = 0.5, C_l = 0.1$. Skin friction represents the shear stress exerted by the fluid on a boundary. In blood flow, it influences endothelial cell response and vascular resistance. The definition of D_f is the dimensionless parameter that quantifies the effect of mass flux due to temperature gradients in a fluid. It represents the contribution of thermal diffusion to species transport. In biological flows, the Dufour effect plays a significant role in heat transfer influenced by solute concentration

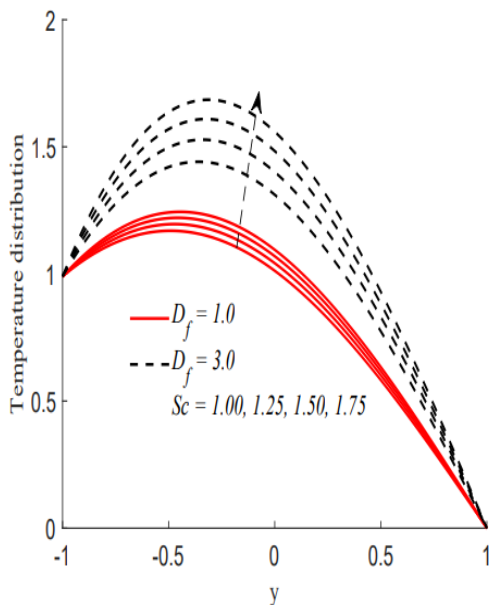


Figure 9: Influence of D_f, Sc on $\theta(y, t)$

variation. As D_f increases, skin friction increases. It is clearly noted that a stronger D_f enhances momentum transfer, which could lead to higher shear stress at the vessel walls. Schmidt number (Sc) is defined as the ratio of momentum diffusivity (kinematic viscosity) to mass diffusivity. A higher Schmidt number implies lower mass diffusivity. The presence of different Schmidt number ($Sc = 1.00, 1.50, 2.00$) indicates varying diffusivity. Higher values of Sc mean lower mass diffusion which lead to an increase in C_f . It is noted that in blood plasma and cellular transport, where lower diffusivity may increase resistance to flow.

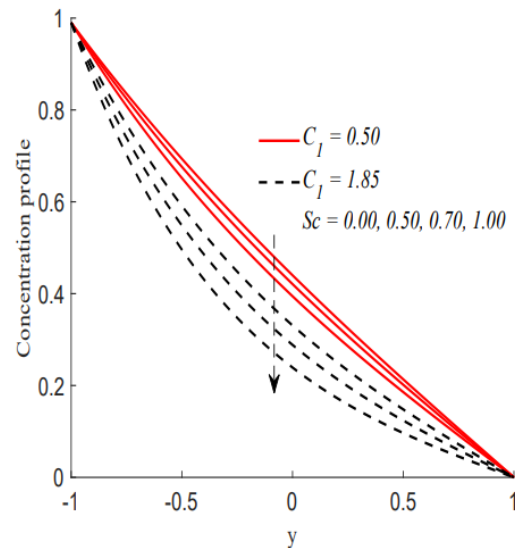


Figure 10: Influence of Sc, C_l on $u(y, t)$

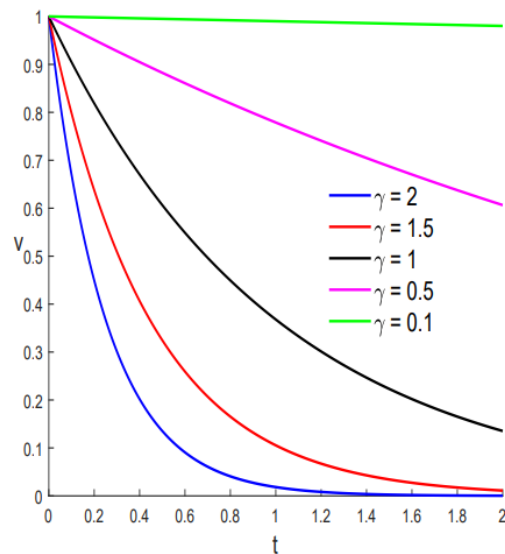


Figure 11: Behaviour of t, γ on normal velocity

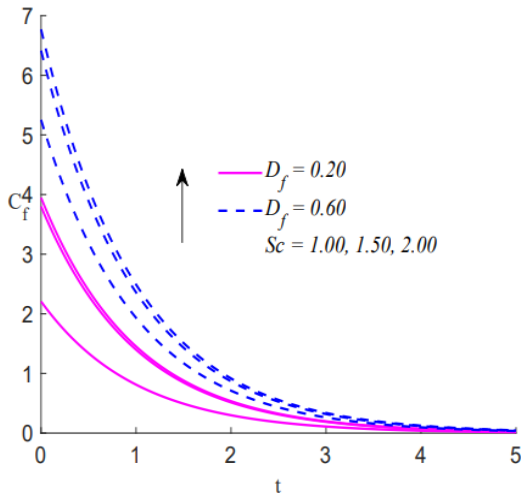


Figure 12: Behaviour of Sc, D_f on Skin Friction

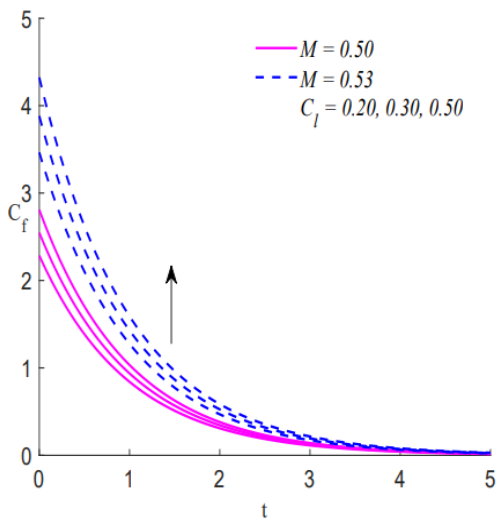


Figure 13: Behaviour of M, C_l on Skin Friction

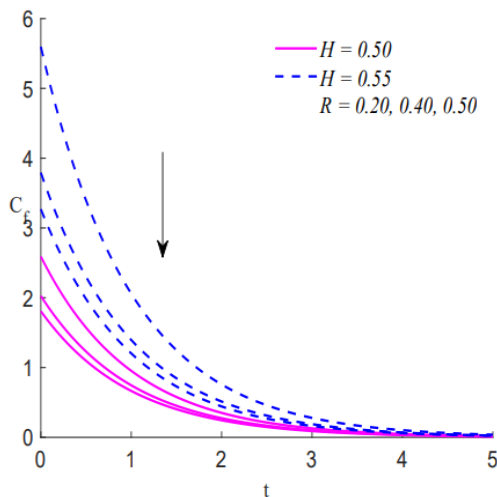


Figure 14: Behaviour of H, R on Skin Friction

Figure (13), the coefficient of skin friction (C_f) for values of $M = 0.5, M = 0.55$ with varying values of C_l is displayed having the parameters, $H = 0.5, Sc = 0.5, D_f = 0.2$. As M increases, the magnetic drag force becomes more dominant, significantly increasing the velocity gradient at the wall and thereby increasing C_f . With increasing C_l , the skin friction coefficient progressively increases.

In Figure (14), the behaviour of the magnetic parameter (M), Dufour number (D_f) on skin friction (C_f) as a function of time (t) for magnitudes of $M = 0.5$ and $M = 0.55$ with varying values of D_f is plotted having the parameters $Sc = 0.5, D_f = 0.2, C_l = 0.1$. Heat source (H) represents energy addition due to an external or internal heat generation source. In blood flow, heat sources can be metabolic processes, external heating such as hyperthermia treatment, viscous dissipation etc. Increasing H increases skin friction, this indicates that the higher heat generation leads to enhanced shear stress at the boundary. Thermal radiation (R) quantifies heat transfer via radiative effect. In biofluids, radiation heat transfer can be applicable in hyperthermia therapy, laser treatment, and physiological thermoregulation. Higher radiation contributes to more heat transfer which increase temperature gradient and it leads to enhance velocity near the wall and greater shear stress.

In Figure (15), the influence of time (t), Dufour number (D_f), Prandtl Number (Pr) over Nusselt Number (Nu) is presented for $D_f = 0.1$ and $D_f = 1.0$ with different values of Pr . The Nusselt number (Nu) represents the ratio of thermal energy convected to thermal energy conducted across the blood flow boundary. Convection has a compromise between advection and molecular diffusion. The Nusselt number (Nu) can be defined as the ratio of convective heat transfer to conductive heat transfer. So, conductive heat transfer dominates over convective heat transfer due to the turbulent blood flow. It is perceived that Nu is inversely proportional to both Pr and D_f . As Pr increases, the thermal boundary layer thickens by reducing heat transfer efficiency and instantly decreasing Nu . For higher dissimilar D_f values diminish convective heat transfer, further reducing Nu . In addition, Nusselt number approaches zero over time (t). This clearly indicates that a steady-state condition where convective and conductive heat transfer mechanisms balance out.

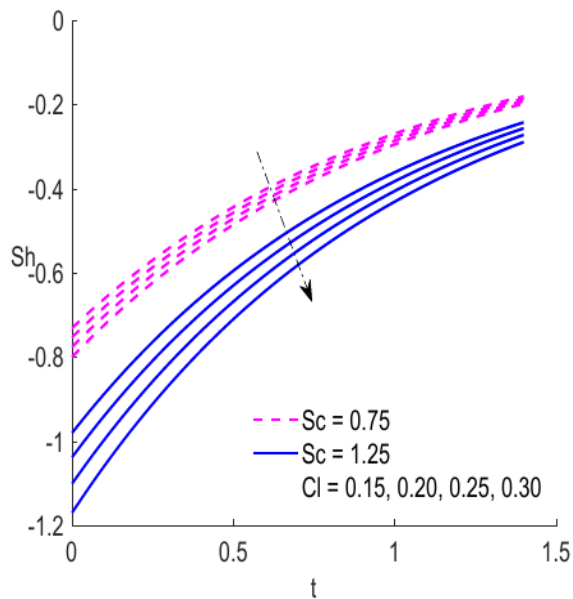


Figure 15: Behaviour of Sc, C_l on Nusselt Number

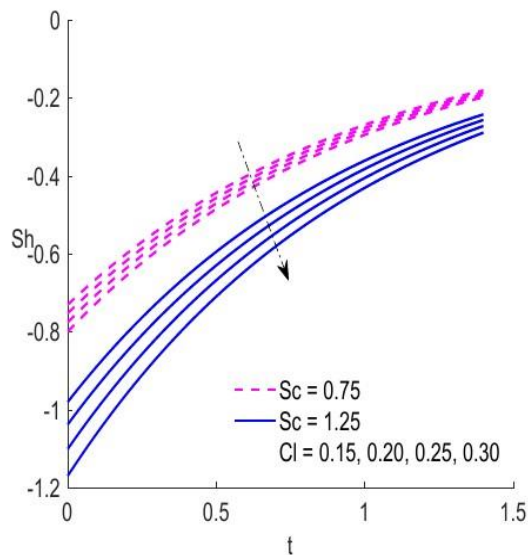


Figure 16: Behaviour of Sc, C_l on Sherwood Number

In Figure (16), the influence of time (t), the chemical reaction parameter (C_l) and the Schmidt number (Sc) on the Sherwood number (Sh) are examined for $Sc = 0.75$ and $Sc = 1.25$, with varying C_l . The Sherwood number (Sh) is a dimensionless quantity used in mass transfer operations that describes the ratio of convective mass transfer to mass diffusivity. It also represents the mass transfer coefficient for transport from a moving fluid to a cluster of spherical particles particularly in system with high porosity. The Sherwood number is commonly used in cases where the Schmidt number is present. The results indicate that the enhancement in the chemical reaction parameter and Schmidt number leads to reduce the

Sherwood number over time.

CONCLUSIONS

The flow model has been analytically solved by means of regular perturbation technique. The behaviour of velocity, temperature and concentration profiles in the company of uniform inclined magnetic field are depicted through graphical representations. Furthermore, the skin friction, heat and mass transfer coefficients have been computed at the artery wall. The current research is the generalization of established mathematical model of Eldesoky (2012) on time-dependent flow of blood. The analytical solutions are validated by comparison with numerical solutions. A comparative analysis with the studies of Eldesoky (2012) and Ahmed *et al.*, (2023) —where the Dufour effect is neglected or radiation and reaction are absent, validates the findings. The key findings are summarized as follows:

- The influence of magnetic force, chemical reaction has been notably observed in this blood flow model. The magnetic field parameter reduces the fluid velocity by generating a Lorentz force. An increase in chemical reaction decreases fluid motion, thereby slowing the axial velocity.
- As values of Dufour number increase at low magnetic parameter, the phenomenon reduces the resistance to flow and enhances the velocity field by introducing thermal energy.
- It is illustrated that the diminution in thermal radiation leads to rise the axial velocity by reducing the flow within the arterial layers the particles are of huge mass diffusivity.
- As Prandtl number decreases then the velocity of the blood exhibits Newtonian behaviour, laminar flow (i.e., parabolic about $y = 0$) and the velocity shrinks near the wall by increasing thermal gradient which leads a stable flow.
- The temperature distribution becomes lower across the region with increasing Prandtl number as result of the dispersal thermal diffusivity whereas the enhancement in Dufour number and heat source increase the temperature due to the sudden domination of momentum diffusivity.
- It is observed that the increase in Dufour number leads to higher skin friction due to increased energy transfer from mass diffusion.
- Negative Nusselt number indicates heat transfer is predominantly governed by convection, rather than the expected conduction.

- Negative Sherwood number indicates a reversal of the typical mass transfer behaviour, where convection becomes the dominant mechanism over diffusionspecie concentration on natural convection flow through a channel.

REFERENCES

Adhikary, S.D. and Misra, J.C. (2011). Unsteady two-dimensional hydromagnetic flow and heat transfer of a fluid. *International Journal of Applied Mathematics and Mechanics*, 7(4): 1–20.

Ahmed, K.K., Ahmed, S. and A. J. Chamkha. (2023). Impact of Inclined Magnetic Force on Bio-Fluid in Permeable Bifurcated Arteries: Analytical Approach. *Journal of Nanofluids*, 12(2):332–340, ISSN 2169-432X. doi:10.1166/jon.2023.2000. URL <https://www.ingentaconnect.com/content/10.1166/jon.2023.2000>.

Chakravarty, S. and Sen, S. (2005). Dynamic response of heat and mass transfer in blood flow through stenosed bifurcated arteries. *Korea-Australia Rheology Journal*, 17 (2):47–62.

Das, K and Saha, G.C. (2009). Arterial mhd pulsatile flow of blood under periodic body acceleration. *Bulletin of Society of Mathematicians Banja Luka*, 16:21–42.

Eckert, R.G. and Drake Jr R.M. (1987). *Analysis of heat and mass transfer*.

Eldesoky, I.M. (2012). Mathematical analysis of unsteady mhd blood flow through parallel plate channel with heat source. In *The International Conference on Mathematics and Engineering Physics*, volume 6, pages 1–16. Military Technical College, URL <https://dx.doi.org/10.1007/s12668-019-00651-x>.

Eldesoky, I.M., Abdelsalam, S.I., El-Askary, W.A., El-Refaey, A.M. and MM Ahmed. (2019). Joint effect of magnetic field and heat transfer on particulate fluid suspension in a catheterized wavy tube. *BioNanoScience*, 9:723–739. URL <https://dx.doi.org/10.1007/s12668-019-00651-x>.

Granot, Y. and Rubinsky, B. (2008). Mass transfer model for drug delivery in tissue cells with reversible electroporation. *International Journal of Heat and Mass Transfer*, 51(23-24):5610–5616. ISSN 00179310. doi:10.1016/j.ijheatmasstransfer. 2008.04.041. URL <https://linkinghub.elsevier.com/retrieve/pii/S001793100800272x>.

Hamza, M.M., Isa, M.M., Ibrahim, Y. and Usman, H. (2024). Analysis of magnetized chemical reaction under

arrhenius control in the presence of navier slip and convective boundary conditions. *Journal of Basics and Applied Sciences Research*, 2(2):71–82, doi:<https://doi.org/10.33003/jobasr-2024-v2i2-54>.

Hayat, T., Shehzad, S.A. and Alsaedi, A. (2012). Soret and dufour effects on magnetohydrodynamic (mhd) flow of casson fluid. *Applied Mathematics and Mechanics*, 33:1301–1312.

Ibrahim, Y., Adamu, I., Ibrahim, U.T. and Sa'adu A. (2024). Influence of thermal diffusion (soret term) on heat and mass transfer flow over a vertical channel with magnetic field in tensity. *Journal of Basics and Applied Sciences Research*, 2(2):60–70, ISSN 3026-9091, ISSN (online): 1597-9962. doi:<https://doi.org/10.33003/jobasr-2024-v2i2-53>.

Jain, M., Sharma, G.C. and Atar Singh. (2009). Mathematical analysis of mhd flow of blood in very narrow capillaries (research note). *International Journal of Engineering Transactions B: Applications*, 22(3):307–315.

Jamali M.S., and Ismail, Z. (2019). Simulation of heat transfer on blood flow through a stenosed bifurcated artery. *Journal of Advanced Research in Fluid Mechanics and Thermal Sciences*, 60(2):310–323.

Jha B.K. and Gambo, Y.Y. (2019). Dufour effect with ramped wall temperature and specie concentration on natural convection flow through a channel. *International Journal of Applied Mechanics and Engineering*, 1(1):111–130.

Korchevskii, E.M. and Marochnik, S.L. (1965). Magnetohydrodynamic version of movement of blood. *Biophysics*, 10(2):411–414.

Kumar, D., Satyanarayana, B., Kumar, R., Kumar, S. and Deo N. (2021). Application of heat source and chemical reaction in mhd blood flow through permeable bifurcated arteries with inclined magnetic field in tumor treatments. *Results in Applied Mathematics*, 10:100151. URL <https://dx.doi.org/10.1016/j.rinam.2021.100511>

Lagendijk, J.J.W. (1982). The influence of bloodflow in large vessels on the temperature distribution in hyperthermia. *Physics in Medicine and Biology*, 27(1):17, doi:10.1088/0031 9155/27/1/002.

LathaR. and Kumar, B.R. (2016). Mass transfer effects on unsteady mhd blood flow through parallel plate channel with heat source and radiation. *JAEBS*, 6(5):96–106.

- Misra, J.C. and Ghosh S.K. (1997). A mathematical model for the study of blood flow through a channel with permeable walls. *Acta mechanica*, 122:137–153.
- Necati, M. K. (1985). *Heat transfer: a basic approach*. McGraw-Hill, New York. ISBN 9780070479821. URL <https://zbib.org/80c4e0edf6794439a64f6b5c912033c4>.
- Omamoke, E., Amos, E. and Jatari, E. (2020). Impact of thermal radiation and heat source on mhd blood flow with an inclined magnetic field in treating tumor and low blood. *Asian Research Journal of Mathematics*, 16(9): 77–87. URL <https://dx.doi.org/10.9734/arjom-2020-v16i930221>.
- Platten, J.K. (2006). The sores effect: a review of recent experimental results. *Journal of Applied Mechanics*, 73(1):1–15.
- Prakash, O.M., Singh, S.P., Kumar, D. and Dwivedi, Y.K. (2011). A study of effects of heat source on mhd blood flow through bifurcated arteries. *AIP Advances*, 1(4).
- Ramamurthy G. and Shanker B. (1994.). Magnetohydrodynamic effects on blood flow through a porous channel. *Medical and Biological Engineering and Computing*, 32:655–659, doi:10.1007/BF02524242.
- Reddy G.V.R. (2016). Soret and dufour effects on mhd free convective flow past a vertical porous plate in the presence of heat generation. *International Journal of Applied Mechanics and Engineering*, 21(3):649–665.
- Sanyal D.C. and Biswas, A. (2010). Pulsatile motion of blood through an axisymmetric artery in presence of magnetic field. *Assam University Journal of Science and Technology*, 5(2):12–20.
- Sanyal, D.C., Das, K. and Debnath, S. (2007). Effect of magnetic field on pulsatile blood flow through an inclined circular tube with periodic body acceleration. *Journal of Physical Science*, 11:43–56.
- Sharma, G.C., Jain, M. and Kumar A. (2004). Performance modeling and analysis of blood flow in elastic arteries. *Mathematical and computer modelling*, 39(13):1491–1499.
- Sharma, M. Sharma, B.K., Gaur, R.K. and Bhavya Tripathi. (2019). Soret and dufour effects in biomagnetic fluid of blood flow through a tapered porous stenosed artery. *Journal of Nanofluids*, 8(2):327–336.
- Shit, G.C. and Roy M. (2016). Effect of induced magnetic field on blood flow through a constricted channel: An analytical approach. *Journal of Mechanics in Medicine and Biology*, 16 (03):1650030.
- Shukla, A.K., Dwivedi, Y.K. and Mohammad Suleman Quraishi. (2022). A numerical simulation of sores-dufour effect on unsteady mhd casson fluid flow past a vertical plate with hall current and viscous dissipation.
- Singh, J. and Rathee R. (2010). Analytical solution of two-dimensional model of blood flow with variable viscosity through an indented artery due to ldl effect in the presence of magnetic field. *International Journal of Physical Sciences*, 5(12):1857–1868.
- Srinivasacharya, D. and Rao G.M. (2016). Mathematical model for blood flow through a bifurcated artery using couple stress fluid. *Mathematical biosciences*, 278:37–47.
- Suri, P.K. and Suri, P.R. (1981). Effect of static magnetic field on blood flow in a branch. *Indian J. pure appl. Math*, 12(7):907–918.
- Tzirtzilakis, E.E. (2005). A mathematical model for blood flow in magnetic field. *Physics of fluids*, 17(7), doi:10.1063/1.1978807.
- Varshney, G., Katiyar, V. and Sushil Kumar. (2010). Effect of magnetic field on the blood flow in artery having multiple stenosis: a numerical study. *International Journal of Engineering, Science and Technology*, 2(2):967–82.
- Verma, N. and Parihar, R.S. (2009). Effects of magneto-hydrodynamic and hematocrit on blood flow in an artery with multiple mild stenosis. *International Journal of Applied Mathematics and Computation*, 1(1):30–46
- Wang, C.Y. (2008). Heat transfer to blood flow in a small tube. *Journal of Biochemical Engineering*, 130(2):024501. URL <https://dx.doi.org/10.1115/1.2898722>.
- White, F.M. (2006). *Viscous fluid flow*. McGraw-Hill series in mechanical engineering. McGraw-Hill Higher Education, New York, NY, 3rd ed edition. ISBN 9780072402315. URL <https://zbib.org/17c162d7bb2e4d0484760e07cbb50aa6>.
- Zamir, M. and Roach M.R. (1973). Blood flow downstream of a two-dimensional bifurcation. *Journal of Theoretical Biology*, 42(1):33–48, doi:10.1016/0022-5193(73)90146-x.

Appendix A

NOMENCLATURE

G	Constant
Sc	Schmidt number
Pr	Prandtl number
k	Thermal conductivity
C_p	Heat capacity
Q	Heat quantity
B_0	Magnetic field intensity
M	Magnetic field
Nu	Nusselt number
T	Dimensional temperature
T_0	Wall temperature
g	Gravitational acceleration
D^*	Dimensional Dufour parameter
D_f	Dufour Number
D	Diffusion coefficient
t'	Dimensional time
t	Dimensionless time
p'	Dimensional pressure
u	Velocity in the x-direction
v	Velocity in the y-direction
C_f	Skin friction
f	Dimensionless pressure
d	Channel diameter
Re	Magnetic Reynold's number
q_r	Radiative heat flux
\bar{v}	Mean velocity
$\frac{1}{n_p}$	Porosity parameter
m	Rate of mass flow
R	Thermal radiation parameter
H	Heat source
C_l	Chemical reaction
k_l	Net diffusion of the drug
k'	Roseland's mean absorption coefficient

Greek Symbols

ρ	Density of blood
α	Thermal diffusivity
η	Kinematic viscosity
φ	Dimensionless concentration
θ	Dimensionless temperature
σ	Electrical conductivity
γ	Decay rate parameter
μ	Dynamic viscosity
δ	Stefan-Boltzmann constant
β	Thermal expansion
β_0	Concentration expansion

Appendix B

$$\begin{aligned} \hbar &= \frac{f}{e^{-\gamma^2 t}}, \\ a_1 &= M^2 \sin^2 \varphi \frac{1}{n_p} + , \\ a_2 &= G(\text{constant}) \\ a_3 &= \frac{1}{\eta Pr} + R, \\ a_4 &= \frac{H}{\eta Pr}, \\ a_5 &= \frac{D_f}{\eta Pr}, \\ a_6 &= \frac{a_5}{a_3}, \\ a_7 &= \sqrt{(\gamma^2 - C_l)Sc}, \\ a_8 &= \sqrt{\frac{\gamma^2 + a_4}{a_3}}, \\ a_9 &= \sqrt{\gamma^2 - a_1}, \\ a_{10} &= a_6 a_7^2, \\ a_{11} &= \frac{a_{10}}{2(a_8^2 - a_7^2) \cos a_7}, \\ a_{12} &= \frac{a_{10}}{2(a_8^2 - a_7^2) \sin a_7}, \\ a_{13} &= \frac{1}{2 \cos a_8} [1 - 2a_{11} \cos a_7], \\ a_{14} &= \frac{1}{2 \sin a_8} [1 - 2a_{12} \cos a_7], \\ a_{15} &= \frac{\hbar}{a_2^2}, \\ a_{16} &= \frac{g\beta a_{11}}{a_9^2 - a_7^2}, \\ a_{17} &= \frac{g\beta a_{12}}{a_9^2 - a_7^2}, \\ a_{18} &= \frac{g\beta a_{13}}{a_9^2 - a_8^2}, \\ a_{19} &= \frac{g\beta a_{14}}{a_9^2 - a_8^2}, \\ a_{20} &= \frac{g\beta a_{14}}{2 \cos a_7}, \\ a_{21} &= \frac{g\beta' a_{14}}{2 \sin a_7}, \\ a_{22} &= \frac{1}{2 \cos a_9} [1 - 2a_{15} + a_{16} \cos a_7 + 2a_{18} \cos a_8 \\ &\quad + 2a_{20} \cos a_8], \\ a_{23} &= \frac{1}{2 \sin a_9} [1 + a_{17} \cos a_7 + 2a_{19} \cos a_8 \\ &\quad - 2a_{21} \cos a_7] \end{aligned}$$